

# Temperature Dependence of the Interaction Parameter between Polystyrene and Poly(methyl methacrylate)

Jörg Kressler, Noboru Higashida, Ken Shimomai, and Takashi Inoue\*

Department of Organic and Polymeric Materials, Tokyo Institute of Technology, Ookayama, Meguro-ku, Tokyo 152, Japan

Toshiaki Ougizawa

Polymer Processing Laboratory, National Institute of Materials and Chemical Research, Tsukuba, Ibaraki 305, Japan

Received March 23, 1993; Revised Manuscript Received February 1, 1994\*

**ABSTRACT:** The temperature dependence of the interaction parameter  $\chi$  between polystyrene and poly(methyl methacrylate) was studied by means of cloud point and PVT measurements. With these data the phase diagrams and the temperature dependence of  $\chi$  were calculated using the classical Flory–Huggins theory, the equation-of-state theory of Flory, Orwoll, and Vrij, and a modified cell model by Dee and Walsh. The results obtained from all three theories are very similar, suggesting that the free volume contributions in the system under investigation are of minor influence. The comparison between obtained data and literature data of absolute values of  $\chi$  is very difficult because a number of model-dependent quantities, such as segment length or segment volume, influence the results. Thus it is always better to compare the temperature dependence of  $\chi$ . However, also in this case model parameters can lead to different  $\chi(T)$  functions as shown for the examples of the determination of  $\chi(T)$  from interfacial thickness data and from phase diagrams using equation-of-state theories.

## Introduction

There are only a few values of experimentally determined positive polymer–polymer interaction parameters  $\chi$  because of difficulties in measuring them. When data are available, they are usually taken at a fixed temperature. The system polystyrene/poly(methyl methacrylate) (PS/PMMA) might be an exception, because a relatively large number of  $\chi$  values for one temperature as well as temperature-dependent data are known. Here the problem is the wide scattering of the measured  $\chi$  parameters, and, concerning the temperature dependence, results are completely contradictory. Isothermal measurements of  $\chi$  carried out by using a number of different methods and at different temperatures gave values in the range 0.0044–0.032.<sup>1</sup> Thus the scattering of the values severely limits their practical use. The situation becomes even more disastrous if one compares the temperature dependence of the  $\chi$  parameter reported in the literature. Neutron scattering from block copolymers with relatively low molecular weight in the homogeneous state using random phase approximation gave a result of  $\chi$  being nearly temperature independent,<sup>1</sup> whereas SAXS measurements gave a slightly stronger temperature dependence.<sup>2</sup> Recently, ellipsometric measurements<sup>3</sup> showed that the  $\chi$  parameter decreases with increasing temperature. This is in agreement with early calculations by Patterson et al.<sup>4</sup> using a Prigogine–Flory expression for  $\chi$ . The ellipsometric measurements predict UCST (upper critical solution temperature) behavior for oligomers of styrene and methyl methacrylate which is consistent with a UCST-type phase behavior for the microdomain equilibrium in block copolymers of styrene and methyl methacrylate.<sup>1</sup> In contrast, investigating the phase behavior of thin films of random copolymer blends cast at different temperatures, Braun et al.<sup>5</sup> calculated an exponential increase of the  $\chi$  parameter with temperature, predicting LCST (lower critical solution temperature) behavior.

To interpret the contradictory results, we carried out PVT (pressure–volume–temperature) measurements as well as cloud point measurements on oligomers of styrene and methyl methacrylate. Cloud point measurements are a convenient method to obtain phase diagrams which can then be fitted by suitable thermodynamic theories.<sup>6,7</sup> Using the classical Flory–Huggins (FH) theory, the equation-of-state (EOS) theory of Flory, Orwoll, and Vrij (FOV), and a modified cell model by Dee and Walsh (MCM), we calculate the temperature dependence of the  $\chi$  parameter and phase diagrams and compare them with data from cloud point measurements as well as literature data.

## Theoretical Background

**Flory–Huggins (FH) Theory.** A convenient starting point for the thermodynamic description of polymer blends is the Flory–Huggins equation<sup>8</sup>

$$\frac{\Delta G^M}{RTV} = \frac{\phi_1}{V_1} \ln \phi_1 + \frac{\phi_2}{V_2} \ln \phi_2 + \phi_1 \phi_2 \frac{\chi}{V_r} \quad (1)$$

where  $\Delta G^M$  is the Gibbs free energy of mixing and  $R$  is the gas constant.  $V$  and  $V_r$  are the total and the reference volumes, respectively. The first two terms of the right-hand side of eq 1 represent the combinatorial entropy of mixing where  $\phi_i$  is the volume fraction and  $V_i$  is the volume of a polymer chain of component  $i$ . The third term contains the interaction parameter  $\chi$  which generally takes into account all contributions to the free energy which are not given by the combinatorial entropy. The  $\chi$  parameter was originally defined by Flory and Huggins as  $z\Delta w_{12}/(kT)$ , where  $z$  is the coordination number,  $\Delta w_{12}$  is the exchange energy per contact, and  $k$  is the Boltzmann constant, and is referred to as  $\chi_{FH}$ . This definition is slightly different from the original  $\chi_1$  parameter defined by Flory for polymer solutions. To obtain  $\chi_1$  it is necessary to multiply  $\chi$  by the number of solvent molecules. It can be seen that  $\chi$  is the crucial quantity for the thermodynamic description of phase behavior in polymer blends. The critical values can be found from eq 1 by the condition

\* To whom correspondence should be addressed.

† Abstract published in *Advance ACS Abstracts*, March 15, 1994.

that the second and the third derivatives of  $\Delta G^M$  with respect to the composition are zero. Thus the critical  $\chi$  parameter,  $\chi_{cr}$ , is given by

$$\frac{\chi_{cr}}{V_r} = \frac{1}{2} \left( \frac{1}{V_1^{1/2}} + \frac{1}{V_2^{1/2}} \right)^2 \quad (2)$$

It should be mentioned that for the derivation of eq 2, the assumption of a concentration-independent interaction parameter is made and volume changes do not occur during the mixing.

**EOS of Flory, Orwoll, and Vrij (FOV).** This EOS is given by<sup>9</sup>

$$\frac{\tilde{P}_i \tilde{V}_i}{\tilde{T}_i} = \frac{\tilde{V}_i^{1/3}}{\tilde{V}_i^{1/3} - 1} - \frac{1}{\tilde{T}_i \tilde{V}_i} \quad (3)$$

where  $\tilde{P}_i = P/P_i^*$ ,  $\tilde{V}_i = V_{i,sp}/V_{i,sp}^*$ , and  $\tilde{T}_i = T/T_i^*$  are the reduced pressure, volume, and temperature and the starred quantities are the characteristic or hard-core parameters of component  $i$  and can be obtained from PVT measurements as will be outlined in the Experimental Section. For the mixture it is assumed that the FOV EOS can also be applied and that the hard-core mer volumes are equal,  $v^* = v_1^* = v_2^*$ . With an appropriate EOS expression for the free parameter  $\chi$ , the Gibbs free energy of mixing is then given by<sup>10,11</sup>

$$\begin{aligned} \frac{\Delta G^M}{kT} = & N_1 \ln \phi_1 + N_2 \ln \phi_2 + \frac{rNv^*}{kT} \left[ \phi_1 P_1^* \left( \frac{1}{\tilde{V}_1} - \frac{1}{\tilde{V}} \right) + \right. \\ & \phi_2 P_2^* \left( \frac{1}{\tilde{V}_2} - \frac{1}{\tilde{V}} \right) + 3\phi_1 P_1^* \tilde{T}_1 \ln \frac{\tilde{V}_1^{1/3} - 1}{\tilde{V}^{1/3} - 1} + \\ & \left. 3\phi_2 P_2^* \tilde{T}_2 \ln \frac{\tilde{V}_2^{1/3} - 1}{\tilde{V}^{1/3} - 1} + \frac{\phi_1 \theta_2 X_{12}}{\tilde{V}} \right] \quad (4) \end{aligned}$$

where the first two terms represent the combinatorial entropy of mixing as in the FH equation and  $N$  is the number of polymer chains given by  $N = N_1 + N_2$ . The number of segments  $r$  is given by  $r = x_1 r_1 + x_2 r_2$ , with  $x_1 = N_1/N = 1 - x_2$ . Furthermore, the following relations are used:

$$V^* = r_1 N_1 v_1^* + r_2 N_2 v_2^* = rNv^* \quad (5)$$

$$\theta_2 = s_2 r_2 N_2 / (srN) \quad (6)$$

$$s = \phi_1 s_1 + \phi_2 s_2 \quad (7)$$

where  $\theta_i$  is the site fraction of component  $i$  and  $s$  is the number of contact sites per segment. The ratio  $s_1/s_2$  for the system PS/PMMA was estimated by using Bondi's method<sup>12</sup> to be 0.83.  $X_{12}$  is the exchange energy parameter and can be obtained, e.g., by calorimetric measurements or by fitting to a known phase diagram. Then the chemical potential  $\Delta\mu$  is given by

$$\Delta\mu_1 = \mu_1 - \mu_1^0$$

$$\begin{aligned} = & \left( \frac{\partial \Delta F^M}{\partial N_1} \right)_{T,V,V_1,N_2} + \left( \frac{\partial \Delta F^M}{\partial V} \right)_{T,V,N_1,N_2} \left( \frac{\partial \tilde{V}}{\partial N_1} \right)_{T,V,N_2} + \\ & \left( \frac{\partial \Delta F^M}{\partial \tilde{V}_1} \right)_{T,V,N_1,N_2} \left( \frac{\partial \tilde{V}_1}{\partial N_1} \right)_{T,V,N_2} \\ = & kT [\ln \phi_1 + (1 - r_1/r_2)\phi_2] + r_1 P_1^* v_1^* \times \\ & \left[ 3\tilde{T}_1 \ln \frac{\tilde{V}_1^{1/3} - 1}{\tilde{V}^{1/3} - 1} + \tilde{P}_1 (\tilde{V} - \tilde{V}_1) + \left( \frac{1}{\tilde{V}_1} - \frac{1}{\tilde{V}} \right) + \frac{\phi_2 \theta_2 X_{12}}{P_1^* \tilde{V}} \right] \quad (8) \end{aligned}$$

where  $\Delta F^M$  is the Helmholtz free energy of mixing, which is equivalent to the Gibbs free energy of mixing for systems with high density. The binodals can be calculated using eq 8 and the analogous expression for  $\Delta\mu_2$  as well as the equations  $\mu_{1,A} = \mu_{1,B}$  and  $\mu_{2,A} = \mu_{2,B}$ .

Using the framework of the same theory yields the parameter  $\chi_{FOV}$  to be of the form

$$\begin{aligned} \chi_{FOV} = & \frac{V_r^*}{\phi_1 \phi_2 R T} \left[ \phi_1 P_1^* \left( \frac{1}{\tilde{V}_1} - \frac{1}{\tilde{V}} \right) + \phi_2 P_2^* \left( \frac{1}{\tilde{V}_2} - \frac{1}{\tilde{V}} \right) + \right. \\ & \left. 3\phi_1 P_1^* \tilde{T}_1 \ln \frac{\tilde{V}_1^{1/3} - 1}{\tilde{V}^{1/3} - 1} + 3\phi_2 P_2^* \tilde{T}_2 \ln \frac{\tilde{V}_2^{1/3} - 1}{\tilde{V}^{1/3} - 1} + \frac{\phi_1 \theta_2 X_{12}}{\tilde{V}} \right] \quad (9) \end{aligned}$$

where  $V_r^*$  is the hard-core molar volume of a segment. This  $\chi$  parameter is different from the exchange energy parameter defined in the FH theory, because it takes into account also free volume contributions. Therefore, also the temperature dependence of this  $\chi_{FOV}$  parameter might be very different from the prediction using the classical FH theory.

**Modified Cell Model (MCM) by Dee and Walsh.** The MCMEOS<sup>13</sup> differs from the FOV EOS by the application of the Lennard-Jones 6-12 potential and by the introduction of the hexagonal lattice geometry. This results in a geometrical factor  $\gamma$  which differs from 1 of the cubic lattice used in the FOV EOS. The  $\chi_{MCM}$  parameter can be obtained as follows:

$$\begin{aligned} \chi_{MCM} = & \frac{V_r^*}{\phi_1 \phi_2 R T} \left[ 3\phi_1 P_1^* \tilde{T}_1 \ln \frac{\tilde{V}_1^{1/3} - 0.8909q}{\tilde{V}^{1/3} - 0.8909q} + \right. \\ & 3\phi_2 P_2^* \tilde{T}_2 \ln \frac{\tilde{V}_2^{1/3} - 0.8909q}{\tilde{V}^{1/3} - 0.8909q} + \phi_1 P_1^* \left\{ A \left( \frac{1}{\tilde{V}_1^2} - \frac{1}{\tilde{V}^2} \right) - \right. \\ & \left. \frac{B}{2} \left( \frac{1}{\tilde{V}_1^4} - \frac{1}{\tilde{V}^4} \right) \right\} + \phi_2 P_2^* \left\{ A \left( \frac{1}{\tilde{V}_2^2} - \frac{1}{\tilde{V}^2} \right) - \right. \\ & \left. \frac{B}{2} \left( \frac{1}{\tilde{V}_2^4} - \frac{1}{\tilde{V}^4} \right) \right\} + \phi_1 \theta_2 X_{12} \left( \frac{A}{\tilde{V}^2} - \frac{B}{2\tilde{V}^4} \right) \right] \quad (10) \end{aligned}$$

where  $A$  and  $B$  are constant coefficients determined by the geometry of the cell lattice (for hexagonal close packed geometry,  $A = 1.2045$ ,  $B = 1.011$ , and  $\gamma = 1/2^{1/6}$  or 0.8909). The empirical  $q$  value is 1.07.

## Experimental Section

**Materials.** Molecular weight data and sources of all polymers as well as their PVT data are given in Table 1. The calculations of  $P^*$ ,  $V_{sp}^*$ , and  $T^*$  will be discussed below.

**PVT Measurements.** The densities of the samples at 25 °C under atmospheric pressure were measured with an autopycnometer (Micrometrics). The densities of PS and PMMA are

Table 1. Molecular Weight Data, Sources, and Characteristic Parameters (FOV EOS) of All Polymers<sup>a</sup>

polymer	$M_w$	$M_w/M_n$	source	$P^*/\text{MPa}$	$T^*/\text{K}$	$V_{sp}^*/(\text{cm}^3 \text{g}^{-1})$
PS-0.8K	800	1.13	Aldrich	470	7212	0.8457
PS-1.25K	1250	1.11	Scientific Polymer Products	470	7388	0.8412
PS-1.39K	1390	1.06	Scientific Polymer Products	470	7439	0.8397
PMMA-6.35K <sup>b</sup>	6350	1.05	Polymer Standards Services			
PMMA-12K	12000	1.04	Polysciences	600	7748	0.7224

<sup>a</sup> The molecular weight dependences of the characteristic parameters were taken from ref 24. <sup>b</sup> The characteristic parameters of PMMA-6.35K are not significantly different from the values of PMMA-12K.

1.04 and 1.19  $\text{g cm}^{-3}$ , respectively. The Gnomix Research PVT apparatus was described in detail elsewhere.<sup>14</sup> The sample cell was filled with  $\sim 1$  g of polymer and mercury. The cell was closed on one end by a flexible bellows, and the expansion was measured with changing temperature and pressure to determine the volume. In the isothermal mode volume measurements were carried out at fixed pressure intervals (10 MPa) in the range from 0 to 200 MPa. The process was repeated for temperature intervals of  $\sim 10^\circ\text{C}$ . The PVT apparatus had an absolute accuracy of  $10^{-3}$ – $2 \times 10^{-3} \text{ cm}^3 \text{g}^{-1}$  but volume changes of the order of magnitude of  $10^{-4}$ – $2 \times 10^{-4} \text{ cm}^3 \text{g}^{-1}$  could be resolved. To obtain the characteristic or hard-core parameters  $P^*$ ,  $V_{sp}^*$ , and  $T^*$ , the experimental data were fitted to the EOSs. A nonlinear least squares fit was carried out by minimizing the quantity  $S^2$ .<sup>15</sup>

$$S^2 = \sum_i (P_{i,\text{data}} - P_{i,\text{fit}})^2 / (M - 3) \quad (11)$$

where  $M$  is the number of data points,  $P_{i,\text{data}}$  is the measured pressure at a given data set of  $(V, T)$ , and  $P_{i,\text{fit}}$  is the predicted value of the respective EOS.

**Cloud Point Measurements.** Blends were prepared by solvent casting of a 5 wt % solution of total polymer at different blend ratios in tetrahydrofuran on a coverglass at room temperature. The samples were dried in a vacuum oven at  $60^\circ\text{C}$  for 1 day. For the cloud point measurements the films were isothermally annealed for 24 h at every temperature and the phase behavior was checked by optical microscopy and light scattering. Reversibility was usually found but could not be detected at the extreme edges of the phase diagrams and in the case of PS-1.39K/PMMA-12K at temperatures higher than  $200^\circ\text{C}$ , where chain degradation probably occurred over a longer period of time.

## Results and Discussion

To obtain information on the  $\chi$  parameter in the system PS/PMMA, a combination of cloud point measurements and PVT measurements of low molecular weight components was applied. Figure 1 shows an example of a PVT measurement of PS-0.8K. As can be seen, the isobars are almost straight lines except in the low-temperature range, where a glass transition can be observed (solid line). For instance, the glass transition of PS-0.8K at 0 MPa is at  $\sim 25^\circ\text{C}$ . At 200 MPa the  $T_g$  is shifted to  $\sim 80^\circ\text{C}$ . Figure 2 shows the specific volume dependence on the temperature at different pressures for PMMA-12K. A pressure-dependent glass transition (solid line) can clearly be distinguished. For all samples only the data of the liquid state were used to obtain the hard-core parameters by fitting the PVT data to the EOSs as described.

Parts a–c of Figure 3 show the phase diagrams of blends of PS-1.25K/PMMA-6.35K, PS-1.39K/PMMA-6.35K, and PS-1.39K/PMMA-12K. All phase diagrams show UCST behavior. Details of the calculations of the binodals will be discussed below. The phase diagrams of Figures 3a–c depict the binodals obtained by using the FH theory (dashed line) and the binodals obtained by applying the FOV EOS theory (full line) in comparison with the data points from cloud and transparent samples. As can be seen, the experimentally determined area of immiscibility is usually somewhat broader than the calculated binodals.

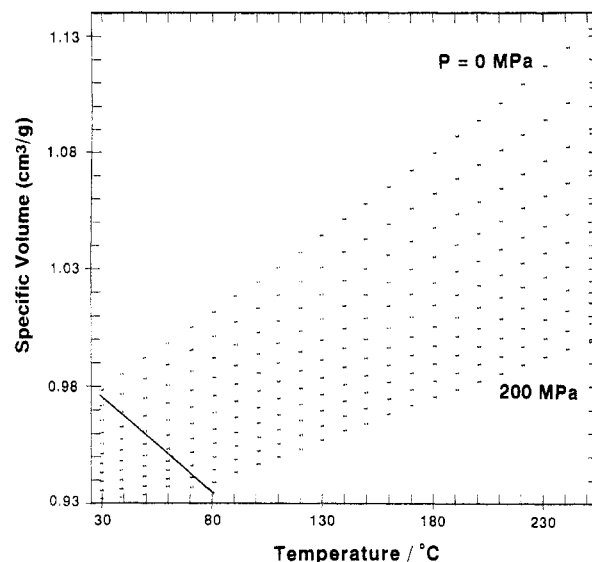


Figure 1. PVT data for PS-0.8K show a nearly linear increase of the specific volume above the glass transition temperature (full line). The bottom isobar was obtained at 200 MPa, the others in steps of 20 MPa.

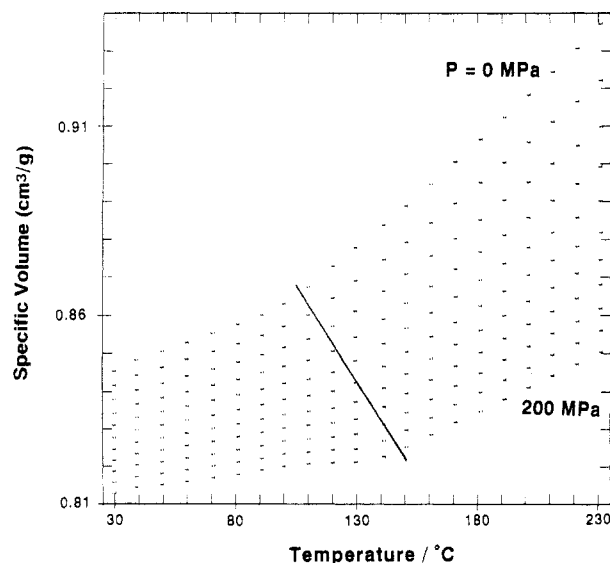
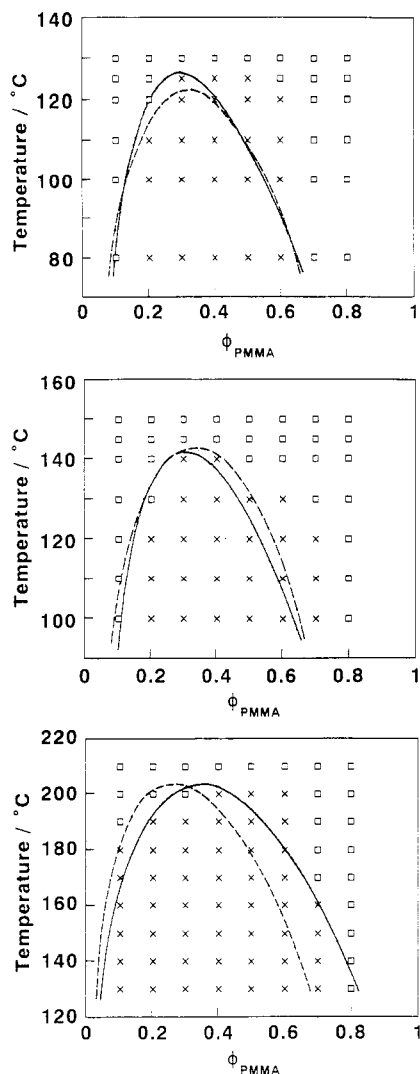


Figure 2. PVT data for PMMA-12K where a pressure-dependent glass transition (full line) can be observed. The isobars range from 200 MPa at the bottom to 0 MPa at the top in steps of 20 MPa.

This is also observed, e.g., in low molecular weight blends of poly(ethylene glycol) with poly(propylene glycol) and polystyrene with polybutadiene.<sup>16</sup> In our case it is obvious that the strongest deviations between cloud point curve and binodal always occur at the higher glass transition side; i.e., at higher PMMA contents the glass transition is always higher because PMMA is always the component with the higher molecular weight. This implies that nonequilibrium effects might be responsible for these deviations. Another contribution to the broadening of the phase diagram may arise from nonclassical contribu-



**Figure 3.** Phase diagrams of PS/PMMA blends; (---) binodals calculated with FH theory; (—) binodals calculated with FOV theory. For calculations using the FH theory, a reference volume of 100 cm<sup>3</sup> was used, and for the FOV theory, a molecular weight of a segment of 100 g mol<sup>-1</sup> was used. (x) Cloud samples; (□) transparent samples. (a) PS-1.25K/PMMA-6.35K; (b) PS-1.39K/PMMA-6.35K; (c) PS-1.39K/PMMA-12K.

tions in the critical region.<sup>17</sup> However, the order of magnitude of these contributions should be smaller compared with the experimentally observed results.

To obtain the binodals from the FH theory, the temperature dependence of  $\chi$  is needed. Under the assumption that the maximum of the cloud point curve is identical with the critical temperature, eq 2 can be used to obtain the  $\chi_{FH}$  parameter at this temperature. This can be seen in Figures 4 and 5 together with a number of different values obtained by EOS approaches and taken from the literature which will be discussed later. The values at 80 and 120 °C are calculated using cloud point curves reported in ref 18. These values are in good agreement under the condition that always a reference volume of 100 cm<sup>3</sup> is chosen. Figure 5 shows that the classical description of  $\chi_{FH} = A + B/T$  can be applied as a good approximation, and in the case under consideration,  $A$  and  $B$  are -0.032 and 48.2, respectively ( $T$  in K). Using the best fit parameter also explains why the calculated critical points by using the FH theory may deviate slightly from the maximum of a cloud point curve. This effect can be seen well in the phase diagram of PS-1.25K/PMMA-6.35K (Figure 3b). Furthermore, by using eqs 9 and 10, respectively, and characteristic parameters, it is possible

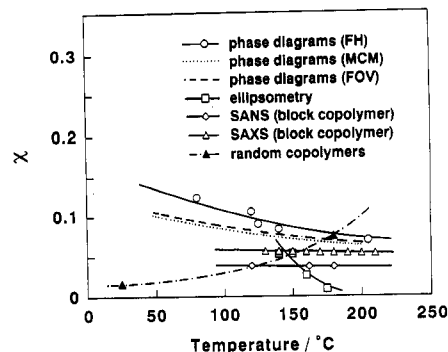


**Figure 4.** Temperature dependence of  $\chi$  obtained by different methods in the system PS/PMMA; phase diagram of oligomers and the FH theory (this paper (○)); the values at 80 and 120 °C are taken from ref 18,  $V_r = 100$  cm<sup>3</sup>, ellipsometry,  $b = 8$  Å (Higashida et al.<sup>3</sup> (□)), FOV theory and phase diagrams of this paper (---), MCM theory (···),  $M_r = 100$  g mol<sup>-1</sup>, SANS (Russell et al.<sup>1</sup> (◇)), SAXS (Stühn<sup>2</sup> (Δ)), and random copolymer blends (Braun et al.<sup>5</sup> (▲)).

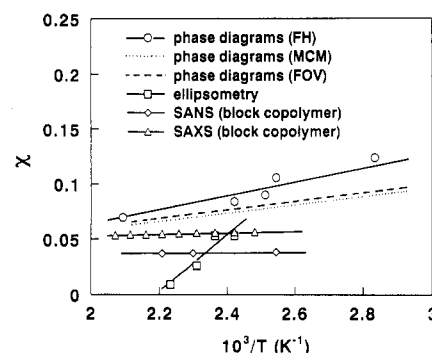


**Figure 5.**  $\chi$  values as seen in Figure 4 plotted versus  $1/T$ .

to calculate the temperature dependence of the  $\chi_{FOV}$  and  $\chi_{MCM}$  parameters applying the outlined EOS theories. It can also be seen that the  $\chi$  parameters obtained from the FOV and MCM EOSs are almost identical because of small free volume differences between PS and PMMA (similar  $T^*$ ).

Another method to calculate the binodals in a context of the FOV EOS theory can be applied by using the expressions of the chemical potentials and the characteristic parameters as discussed in the Theoretical Background section. Here the parameter  $X_{12}$  is fitted to the maximum temperature of the cloud point curve, again under the assumption that this maximum represents the critical temperature. The obtained values of  $X_{12}$  range from 3.08 to 3.35 J cm<sup>-3</sup>. Thus the numerical value is smaller than in the system polystyrene/polybutadiene<sup>16</sup> ( $\sim 7$  J cm<sup>-3</sup>), which means that the repulsive interactions in the system under investigation are smaller. The calculated binodals using both the FOV EOS and FH theories are relatively similar. This can be explained by the fact that the free volume term in the system under consideration does not have a major influence. This is in agreement with the fact that the thermal expansion coefficients and the characteristic temperatures  $T_i^*$  of PS and PMMA are very similar. Stronger deviations between the FH and FOV EOS theories occur only in the system PS-1.39K/PMMA-12K (cf. Figure 3c). It seems to be possible that at higher temperatures EOS effects become more effective.

Furthermore, Figure 6 shows the effect caused by using a different molecular weight of a segment ( $M_r$ ). The temperature dependences of the  $\chi_{FOV}$  parameters obtained by using the three different phase diagrams and one  $M_r$  value are in good agreement. Changing the molecular

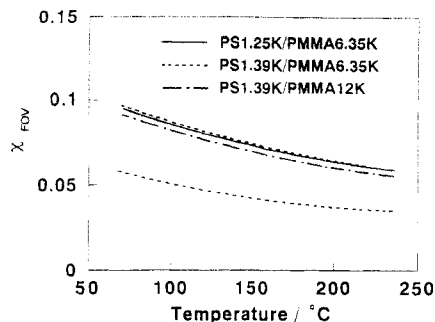


**Figure 6.** Temperature dependence of  $\chi_{FOV}$  between PS/PMMA obtained by using eq 9 and by adjusting  $X_{12}$  to the critical temperatures. PS-1.25K/PMMA-6.35K,  $X_{12} = 3.35 \text{ J cm}^{-3}$ ; PS-1.39K/PMMA-6.35K,  $X_{12} = 3.32 \text{ J cm}^{-3}$ ; PS-1.39K/PMMA-12K,  $X_{12} = 3.08 \text{ J cm}^{-3}$ . The upper three curves were obtained with  $M_r = 100 \text{ g mol}^{-1}$ , and the lower curve for the system PS-1.39K/PMMA-6.35K was obtained using a value of  $M_r = 60 \text{ g mol}^{-1}$ .

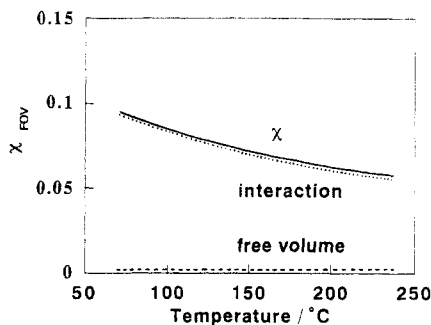


**Figure 7.** Contributions of the free volume term (---) and the interaction term (---) to the  $\chi_{FOV}$  parameter (—) in the system PS-1.39K/PMMA-6.35K ( $M_r = 100 \text{ g mol}^{-1}$ ) (FOV EOS).

weight of a segment from 100 to 60  $\text{g mol}^{-1}$  leads to a smaller  $\chi$  parameter, and also the temperature dependence of  $\chi$  is changed slightly. However, in principle, the temperature dependence is not very different from that obtained by using the FH theory as can be seen in Figures 4 and 5. This again is in agreement with expectations because of the small contributions of EOS effects in the system under investigation, which can also be seen from Figure 7. As outlined above, using EOS theories yields a  $\chi$  parameter consisting of an interaction and a free volume term. Thus the last term in the brackets of eq 9 or 10 takes into account interactions, and the other terms free volume contributions. As already qualitatively discussed, it turns out that the free volume contributions in the system under investigation are nearly negligible, but they increase slightly with temperature.

Finally, we want to compare the reported temperature dependence of  $\chi$  with a number of results given in the literature<sup>1-3,5</sup> and shown in Figures 4 and 5. The literature data were obtained by small-angle neutron scattering,<sup>1</sup> ellipsometry,<sup>3</sup> small-angle X-ray scattering,<sup>2</sup> and random copolymer blends.<sup>5</sup> There are tremendous differences in all reported values. Most values can be replotted as shown in Figure 5 assuming a linear relationship of  $\chi$  versus  $1/T$ .

Only Braun et al. calculated an exponential increase of  $\chi$  with increasing temperature.<sup>5</sup> To obtain these values ternary solutions of the type polymer A/polymer B/solvent were prepared, where A and B were usually one or two random copolymers. The solvent was evaporated at different temperatures, and the resulting phase behavior was interpreted as polymer-polymer phase behavior. Using a mean field theory, it is then also possible to make conclusions about the homopolymer-homopolymer interaction parameter. The crucial point is that the solvent does not influence the phase behavior during the late stage

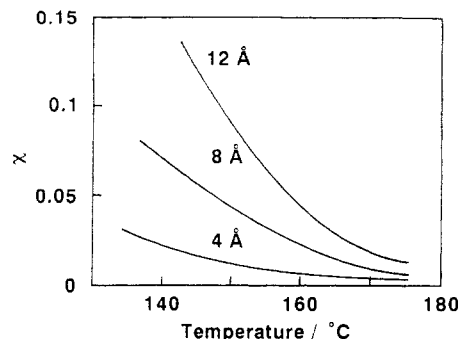


**Figure 8.** Temperature dependence of  $\chi$  for the system PS/PMMA calculated from interfacial thickness data given in ref 3 using eq 12 and different values for the segment length  $b$ .

of evaporation. The result is very questionable because it predicts LCST behavior in blends of PS and PMMA with low molecular weight, and thus it is in disagreement with a number of experimental findings. It is, for example, a well-known fact that block copolymers of styrene and methyl methacrylate display a UCST-type order-disorder transition.<sup>1</sup> This means, in fact, that  $\chi$  must decrease with increasing temperature. The same conclusion can be made from the occurrence of UCST behavior in oligomer blends of styrene and methyl methacrylate which has been discussed here. Early calculations by Patterson et al.<sup>4</sup> using EOS thermodynamics showed also a decreasing  $\chi$  parameter in the temperature range of interest. They used a  $X_{12}$  value of  $10 \text{ J cm}^{-3}$  and the parameter  $\tau = 1 - (T_1^*/T_2^*)$  was set to 0, indicating that the free volume differences between PS and PMMA are very small. The same tendency was found by applying the random phase approximation<sup>19</sup> in one-phase block copolymers of styrene and methyl methacrylate to SANS data.<sup>1</sup> As figured out recently by Dudowicz and Freed,<sup>20</sup> the  $\chi$  parameter determined from block copolymers might be different from that of the corresponding homopolymer blends caused by the junction point. Nevertheless, the temperature dependence of  $\chi$  should be similar. The measured interfacial thickness, determined by ellipsometry,<sup>3</sup> increases with temperature; i.e.,  $\chi$  decreases with temperature in the range of chosen temperatures.

The temperature dependence of  $\chi$  measured by ellipsometry seems to be somewhat stronger than that measured by neutron scattering. This might be caused by the fact that small differences in the interfacial thickness  $\lambda$  result in large differences in the  $\chi$  parameter because of the relation  $\lambda \sim \chi^{-1/2}$ . Furthermore, Figure 8 shows that according to the theory of Broseta et al.,<sup>21</sup> the interfacial thickness not only is a function of the  $\chi$  parameter but also depends very sensitively on the segment length chosen. The  $\chi$  parameter is related to the interfacial thickness  $\lambda$  by<sup>21</sup>

$$\lambda = \frac{2b}{(6\chi)^{1/2}} \left[ 1 + \frac{\ln 2}{\chi} \left( \frac{1}{r_1} + \frac{1}{r_2} \right) \right] \quad (12)$$

where  $b$  is the Kuhn segment length. The Kuhn segment length is an experimentally extremely difficult to handle quantity even if it is well defined within the concept of random walk statistics. The number of segments  $r_i$  was then calculated from the ratio of the overall length of a polymer chain to the segment length  $b$  assuming a planar zigzag conformation. It can also be seen that eq 12 contains only one segment length. Thus an average of the two polymers must be used. Kirste<sup>22</sup> determined from SAXS data a value of  $7.4 \pm 3 \text{ Å}$  for PMMA in solution, and Ballard et al. found a value of  $6.8 \text{ Å}$  for PS.<sup>23</sup> Higashida et al.<sup>3</sup>

used a value of 8 Å for the system PS/PMMA. However, it has to be considered that the segment length might change with a number of influences such as temperature, blend ratio, solvent (or cocomponent in a blend system), etc. Thus to choose a quantity for  $b$  is always somewhat arbitrary.

Similar to the difficulties in random walk statistics, one has to define a reference volume in the FH theory (we used 100 cm<sup>3</sup>). Also for the EOS theories the molecular weight of a segment is necessary because the number of segments is needed for the calculations as can be seen from eqs 9 and 10. A value of 100 g mol<sup>-1</sup>, which was used for the calculations presented, would approximately correspond to a monomer unit of both polymers. However, this value might be too large because it has been found that for PS the molecular weight of a segment should be 57.6 by using the FOV EOS and 23.9 g mol<sup>-1</sup> applying a cell model.<sup>24</sup> Thus a segment would be much smaller than a repeat unit and the absolute values of  $\chi$  would decrease. Thus it becomes difficult to compare absolute values of  $\chi$  obtained by different methods. The temperature dependence of  $\chi$  is also affected but should be comparable within reasonable limits.

## Conclusions

A number of literature data on the interaction parameter  $\chi$  between PS and PMMA were compared with experimental data obtained by using phase diagrams and PVT data. It has been concluded that a comparison of absolute values of  $\chi$  obtained by different methods is nearly impossible because a number of model-dependent quantities are used as segment length or segment volume. Otherwise a comparison of the obtained temperature dependence of  $\chi$  seems to be possible within fair limits. The temperature dependences of  $\chi$  obtained from SANS and SAXS are a little bit less and from ellipsometry a little bit more strong than the presented data obtained from cloud point measurements of oligomers and applying the FH theory as well as two different EOS theories. There

are only small differences in the temperature dependence of  $\chi$  obtained by using the FH theory and from FOV and MCM EOSs, respectively, for blends of PS and PMMA.

**Acknowledgment.** J.K. thanks the Japan Society for the Promotion of Science for supporting his stay at TIT and the Humboldt Foundation for kind help.

## References and Notes

- (1) Russell, T. P.; Hjelm, R. P.; Seeger, P. A. *Macromolecules* **1990**, *23*, 890.
- (2) Stöhn, B. *J. Polym. Sci., Polym. Phys. Ed.* **1992**, *30*, 1013.
- (3) Higashida, N.; Kressler, J.; Yukioka, S.; Inoue, T. *Macromolecules* **1992**, *25*, 5259.
- (4) Patterson, D.; Robard, A. *Macromolecules* **1978**, *11*, 690.
- (5) Braun, D.; Yu, D.; Kohl, P. R.; Gao, X.; Andradi, L. N.; Manger, E.; Hellmann, G. P. *J. Polym. Sci., Polym. Phys. Ed.* **1992**, *B30*, 577.
- (6) Kambour, R. P.; Gundlach, P. E.; Wang, I. C. W.; White, D. M.; Yeager, G. W. *Polym. Commun.* **1988**, *2*, 672.
- (7) Callaghan, T. A.; Paul, D. R. *Macromolecules* **1993**, *26*, 2439.
- (8) Flory, P. J. *Principles of Polymer Chemistry*; Cornell University Press: Ithaca, NY, 1953.
- (9) Flory, P. J.; Orwoll, R. A.; Vrij, A. *J. Am. Chem. Soc.* **1964**, *86*, 3507, 3515.
- (10) Sanchez, I. C. *Polymer Blends*; Paul, D. R.; Newman, S., Eds.; Academic Press: New York, 1978.
- (11) Ougizawa, T.; Inoue, T. *Elastomer Technology Handbook*; Cheremisinoff, N. P., Ed.; CRC Press: Boca Raton, FL, 1993.
- (12) Bondi, A. *J. Phys. Chem.* **1964**, *68*, 441.
- (13) Dee, G. T.; Walsh, D. J. *Macromolecules* **1988**, *21*, 815.
- (14) Zoller, P.; Bolli, P.; Pahud, V.; Ackerman, H. *Res. Sci. Instrum.* **1976**, *49*, 948.
- (15) Dee, G. T.; Walsh, D. J. *Macromolecules* **1988**, *21*, 811.
- (16) Rostami, S.; Walsh, D. J. *Macromolecules* **1985**, *18*, 1228.
- (17) Dudowicz, J.; Lifschitz, M.; Freed, K. F.; Douglas, J. F. *J. Chem. Phys.* **1993**, *99*, 4804.
- (18) Ougizawa, T.; Walsh, D. J. *Polym. J.* **1993**, *25*, 1315.
- (19) Leibler, L. *Macromolecules* **1980**, *13*, 1602.
- (20) Dudowicz, J.; Freed, K. F. *Macromolecules* **1993**, *26*, 213.
- (21) Broseta, D.; Fredrickson, G. H.; Helfand, E.; Leibler, L. *Macromolecules* **1990**, *23*, 132.
- (22) Kirste, R. G. *Makromol. Chem.* **1967**, *101*, 91.
- (23) Ballard, D. G. H.; Wignall, G. D.; Schelten, J. *Eur. Polym. J.* **1973**, *9*, 965.
- (24) Ougizawa, T.; Dee, G. T.; Walsh, D. J. *Polymer* **1989**, *30*, 1675.